

# Reaching for the Stars in the Brain: Polymer-Mediated Gene Delivery to Human Astrocytes

Chaitanya R. Joshi,<sup>1</sup> Vijay Raghavan,<sup>2,3</sup> Sivakumar Vijayaraghavalu,<sup>2</sup> Yue Gao,<sup>2</sup> Manju Saraswathy,<sup>2</sup> Vinod Labhassetwar,<sup>2</sup> and Anuja Ghorpade<sup>1</sup>

<sup>1</sup>Department of Microbiology, Immunology and Genetics, University of North Texas Health Science Center, Fort Worth, TX, USA; <sup>2</sup>Department of Biomedical Engineering, Lerner Research Institute, Cleveland Clinic, Cleveland, OH, USA

**Astrocytes, the “star-shaped” glial cells, are appealing gene-delivery targets to treat neurological diseases due to their diverse roles in brain homeostasis and disease. Cationic polymers have successfully delivered genes to mammalian cells and hence present a viable, non-immunogenic alternative to widely used viral vectors. In this study, we investigated the gene delivery potential of a series of arginine- and polyethylene glycol-modified, siloxane-based polyethylenimine analogs in primary cultured human neural cells (neurons and astrocytes) and in mice. Plasmid DNAs encoding luciferase reporter were used to measure gene expression. We hypothesized that polyplexes with arginine would help in cellular transport of the DNA, including across the blood-brain barrier; polyethylene glycol will stabilize polyethylenimine and reduce its toxicity while maintaining its DNA-condensing ability. Polyplexes were non-toxic to human neural cells and red blood cells. Cellular uptake of polyplexes and sustained gene expression were seen in human astrocytes as well as in mouse brains post-intravenous-injections. The polyplexes also delivered and expressed genes driven by astrocyte-restricted glial fibrillary acidic protein promoters, which are weaker than viral promoters. To our knowledge, the presented work validates a biocompatible and effective polymer-facilitated gene-delivery system for both human brain cells and mice for the first time.**

## INTRODUCTION

Gene-based therapies can address the growing prevalence of neurological diseases and disorders (NDDs). A single, effective gene-delivery system could be used to treat multiple NDDs by altering gene expression of one or more targets, thereby reversing damage and restoring function.<sup>1</sup> Astrocytes, the “star-shaped” glial cells in the brain, are attractive targets for treating NDDs. During homeostasis, astrocytes regulate neurotransmission and synaptic activity by sequestering potassium and neurotransmitters, including glutamate.<sup>2</sup> They have preferential access to therapeutics delivered via the vascular route since their foot processes are integral components of the blood-brain barrier (BBB).<sup>3</sup> Reactive astrogliosis is a hallmark of chronic inflammation characterized by subtle changes to astrocyte structure and function.<sup>4</sup> Due to such diverse characteristics, modu-

lating astrocyte gene expression could benefit a broad spectrum of NDDs. Further, astrocytes secrete several neurotrophic<sup>5,6</sup> and neuro-inflammatory mediators.<sup>7–9</sup> Thus, astrocyte-targeted gene therapy could be used to upregulate neurotrophic factor expression and/or silence that of toxic mediators. To avoid off-target effects on other brain cells, targeted gene delivery could be implemented by using astrocyte-restrictive promoters such as glial fibrillary acidic protein (GFAP),<sup>10</sup> glutamate transporter-1, excitatory amino acid transporter 2,<sup>11</sup> and aldehyde dehydrogenase 1 L1.<sup>12</sup>

Gene delivery to astrocytes or any other cell type in the brain is contingent upon availability of an effective yet biocompatible gene-delivery system. Few viral vector-based therapies for Alzheimer’s and Parkinson’s diseases that transitioned into clinical trials did not show adequate effectiveness in early phases.<sup>13,14</sup> On the other hand, greater versatility, ability to modulate the polymer composition, and lack of immunogenicity make polymer-based gene-delivery systems more appealing than viral vectors for NDD therapies. Among non-viral gene-delivery systems, cationic polymers and lipids have been extensively tested.<sup>15–17</sup> They bind with the negatively charged DNA and deliver it across negatively charged cellular membrane. Among cationic polymers, polyethylenimine (PEI) is considered as a “gold standard” for transfection, but its use is restricted due to cytotoxicity caused by high cationic charge, disrupting cell membrane integrity.<sup>18,19</sup> Further, PEI interacts with serum proteins *in vivo* and also causes red blood cells (RBCs) aggregation and lysis. Therefore, substantial efforts are required to mitigate PEI toxicity that can also offset its transfection and DNA-condensing abilities. We synthesized a series of siloxane-based PEI analogs, modified by arginine (A), and stabilized with polyethylene glycol (PEG) (P),

---

Received 9 June 2018; accepted 22 June 2018;  
<https://doi.org/10.1016/j.omtn.2018.06.009>.

<sup>3</sup>Present address: Department of Chemistry, Vanderbilt University, Nashville, TN, USA

**Correspondence:** Anuja Ghorpade, Department of Microbiology, Immunology and Genetics, University of North Texas Health Science Center, 3500 Camp Bowie Boulevard, Fort Worth, TX 76107, USA.

**E-mail:** [anuja.ghorpade@unthsc.edu](mailto:anuja.ghorpade@unthsc.edu)



**Table 1. Physicochemical Characteristics of A<sub>n</sub>P<sub>n</sub> Polyplexes**

Polymer Name	MES-NHS Buffer pH	PEI Equivalents	Arginine Equivalents	PEG Equivalents	Polyplex Particle Size (nm)	Variance	Zeta potential (mV)
S1 A <sub>1</sub> P <sub>10</sub>	not adjusted	1	1	10	55.33 ± 0.80	0.249 ± 0.02	28.29 ± 0.16
S1 A <sub>5</sub> P <sub>10</sub>	not adjusted	1	5	10	60.00 ± 1.64	0.297 ± 0.03	23.82 ± 0.29
S1 A <sub>7</sub> P <sub>10</sub>	not adjusted	1	7	10	61.97 ± 1.07	0.214 ± 0.02	27.21 ± 1.45
S2 A <sub>1</sub> P <sub>10</sub>	pre-adjusted	1	1	10	56.8 ± 0.43	0.211 ± 0.01	27.08 ± 1.32
S2 A <sub>5</sub> P <sub>10</sub>	pre-adjusted	1	5	10	60.43 ± 0.05	0.252 ± 0.01	27.9 ± 0.86
S2 A <sub>7</sub> P <sub>10</sub>	pre-adjusted	1	7	10	85.77 ± 7.55	0.332 ± 0.02	24.60 ± 3.12

Polyplex (polymer:pDNA) 2:1 w/w; MES, 2-(N-morpholino)ethanesulfonic acid; PEI, polyethylenimine; PEG, polyethylene glycol. Values represented as mean ± SEM.

collectively referred as A<sub>n</sub>P<sub>n</sub>, in which n denotes molar equivalent (eq) of arginine or PEG per PEI in the composition. Six different polymers were generated that differed in the molar ratio of arginine to PEI used while synthesizing these polymers. In addition, S1 series of polymers denotes where the reaction was carried out without the pH adjustment and S2 series where the pH of the reaction buffers were pre-adjusted (Table 1).

Choosing the most relevant *in vitro* or *in vivo* models to test gene-delivery systems is crucial for proof-of-concept studies. Thus far, gene-delivery investigations have predominantly used rodent-derived primary cells and rodent models,<sup>16,20–23</sup> while primary human brain cells have been seldom tested successfully. Gray and colleagues reported adeno-associated virus 9-based vector preferentially transducing neurons in mice and glia in non-human primates (NHPs).<sup>24</sup> The difference in transduced cell types in rodents versus NHPs was attributed to the difference in timing of gliogenesis of these species.<sup>25</sup> Another study testing adeno-associated virus-based delivery using rodent models reported gene-promoter-dependent changes in transduced cell types.<sup>21</sup> These findings led us to believe that the species of the models tested and gene promoters are critical in achieving translational pre-clinical data. Therefore, in this study, we utilized primary human astrocytes and neurons for *in vitro* testing along with astrocyte-specific promoters. We validated brain transfection potential of polyplexes in mice following intravenous (i.v.) injections. Luciferase reporter plasmids (pLucs) were used to determine gene expression using different polyplexes.

We hypothesized that a balanced composition of the polymer with PEI condensing the DNA, arginine helping the DNA transport across plasma membrane, and PEG providing the stability to the polyplex would be effective in neural cell transfection and *in vivo* brain gene delivery. First, thorough *in vitro* studies were performed to assess transfection levels, bio- and hemocompatibility, cellular uptake, and sustained expression in primary cultures of human neurons and astrocytes using pLuc. The most suitable polymer, which showed highest transfection levels and biocompatibility, was then used to validate *in vivo* brain delivery in mice. Our data convincingly demonstrate an effective, non-viral gene-delivery system for human neural cells as well as rodent models and offer novel opportunities for pre-clinical and clinical options for treating neurodegeneration.

## RESULTS

### Characterization of A<sub>n</sub>P<sub>n</sub> Polymers

Synthesized A<sub>n</sub>P<sub>10</sub> polymers consisted of different molar amounts of arginine used per PEI eq (A<sub>1</sub>, A<sub>5</sub>, and A<sub>7</sub>). Polymers were synthesized by not adjusting (series 1, S1) or adjusting (series 2, S2) the pH of 2-(N-morpholino)ethanesulfonic acid (MES) buffer and phosphate buffer saline (PBS) at 6.5 and 7.2, respectively. MES buffer was used for carboxylic acid activation, and PBS buffer was used for reaction between amino groups and activated carboxylic acid. The polymers and pLuc were mixed in 2:1 weight/weight (w/w) ratio to form polyplexes. The zeta potential (23–29 mV) and particle size (50–90 nm) of all polyplexes were in a narrow range irrespective of the synthesis method or the number of arginine residues.

### A Specific Polymer:pDNA Ratio Achieves Optimal Gene Expression and Biocompatibility in Primary Human Fetal Astrocytes

Human astrocytes were transfected with different w/w ratios S2 A<sub>5</sub>P<sub>10</sub>, and pLuc to evaluate the optimized polymer to plasmid DNA (pDNA) ratio that is biocompatible and yet effective in achieving high levels of transfection (Figure 1). Unmodified PEI was used as a positive control of transfection. Both S2 A<sub>5</sub>P<sub>10</sub> and PEI were complexed with pLuc at w/w ratios of 1:1, 2:1, 4:1, and 8:1, keeping concentration of pLuc constant at 2.5 µg/mL to form polyplexes. Luciferase expression was significantly higher in cells treated with 2:1 w/w ratio than other ratios for both polymer and PEI, respectively (\*p < 0.05, \*\*p < 0.01). Also, S2 A<sub>5</sub>P<sub>10</sub> 2:1 w/w transfection led to higher luciferase activity compared to PEI 2:1 w/w transfection (\*\*p < 0.01) (Figure 1A). In parallel, lactate dehydrogenase (LDH) activity increased in 4:1 and 8:1 S2 A<sub>5</sub>P<sub>10</sub>-treated cells compared to 1:1 S2 A<sub>5</sub>P<sub>10</sub>-treated cells (\*p < 0.05, \*\*p < 0.01). Though LDH activity did not change with increasing polyplex ratio in PEI-treated cells, it was higher in 2:1 PEI compared to 2:1 A<sub>n</sub>P<sub>n</sub>-treated cells (#p < 0.05) (Figure 1B). Metabolic activity, measured as 3-(4,5-dimethylthiazol-2-yl)-2, 5-diphenyl-tetrazolium bromide (MTT) absorbance, did not change in S2 A<sub>5</sub>P<sub>10</sub> polyplex-treated cells with increasing ratios and decreased in 4:1 and 8:1 PEI-treated cells compared to 1:1 PEI-treated cells (\*\*p < 0.01, \*\*\*p < 0.001). Cells treated with PEI showed lower MTT compared to S2 A<sub>5</sub>P<sub>10</sub> at 2:1, 4:1, and 8:1 ratios (#p < 0.05, ##p < 0.01), respectively (Figure 1C). Since 2:1 w/w polyplexes provide higher transfection levels and low cytotoxicity

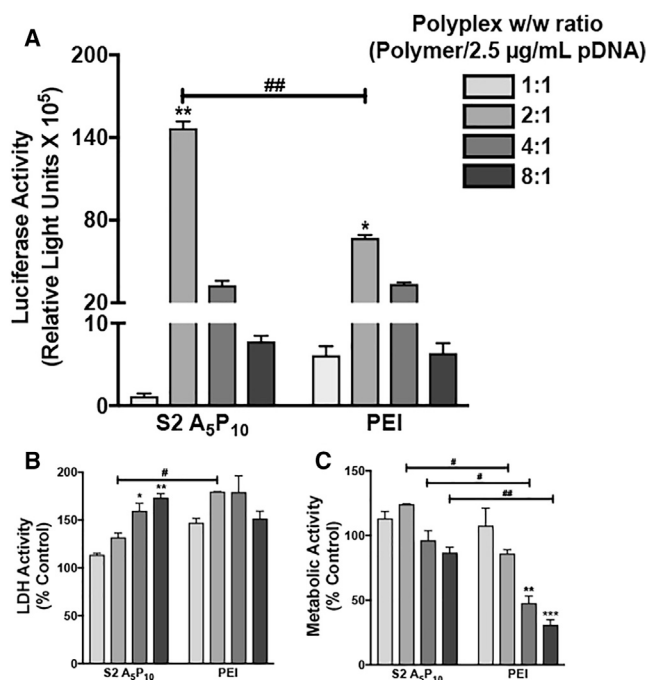


**Figure 1. A Specific Polyplex Ratio Achieves Optimal Gene Expression and Biocompatibility in Primary Astrocytes**

An  $A_nP_n$  analog S2 A<sub>5</sub>P<sub>10</sub> or polyethylenimine (PEI) was mixed with 2.5 μg/mL luciferase plasmid in different w/w ratios (1:1, 2:1, 4:1, and 8:1). Astrocytes (150,000/well) were treated with polyplexes for 3 hr. The polyplex-containing media was removed, and fresh culture medium was added. The (A) luciferase, (B) lactate dehydrogenase (LDH), and (C) metabolic activities were measured 48 hr post-treatment. Data represent mean ± SEM for two donors with a minimum of triplicate determinations/donor (\**p* < 0.05, \*\**p* < 0.01, and \*\*\**p* < 0.001 for 1:1 w/w versus other ratios for S2 A<sub>5</sub>P<sub>10</sub> or PEI, #*p* < 0.05, ##*p* < 0.01 for S2 A<sub>5</sub>P<sub>10</sub> versus PEI at same w/w).

compared to other compositions, further experiments were conducted using this ratio.

#### Physicochemical and/or pH Differences during Polyplex Formulations Alter the Levels of Gene Expression and Biocompatibility in Human Neural Cells

Polyplexes generated from six polymers (S1 A<sub>1</sub>P<sub>10</sub>, S1 A<sub>5</sub>P<sub>10</sub>, S1 A<sub>7</sub>P<sub>10</sub>, S2 A<sub>1</sub>P<sub>10</sub>, S2 A<sub>5</sub>P<sub>10</sub>, and A<sub>7</sub>P<sub>10</sub>) (details in Table 1) were tested for their transfection and biocompatibility in human neural cells. Transfection levels were evaluated by measuring luciferase activity while biocompatibility was assessed with LDH and MTT assays. Polymer effects on cell morphology were determined as an additional indicator of biocompatibility.

In astrocytes, higher gene expression was observed in S2 A<sub>1</sub>P<sub>10</sub> and A<sub>5</sub>P<sub>10</sub> compared to S1 A<sub>5</sub>P<sub>10</sub>, S1 A<sub>7</sub>P<sub>10</sub>, and S2 A<sub>7</sub>P<sub>10</sub> (\**p* < 0.05). A two-way ANOVA revealed that the synthesis method, but not the number of arginine residues, affected transfection levels (\**p* < 0.05 for S1 versus S2) in astrocytes (Figure 2A). None of the six  $A_nP_n$  analogs increased LDH activity compared to controls (Figure 2B).

Metabolic activity was reduced (7%–21%) across polyplex treatments (\**p* < 0.05, \*\*\**p* < 0.001). S1 A<sub>1</sub>P<sub>10</sub> and A<sub>7</sub>P<sub>10</sub> were the most cytotoxic with 21% and 15% decrease in metabolic activity, respectively. S2 polymers presented better biocompatibility as indicated by 7%–12% decrease in metabolic activity (Figure 2C). All polyplexes, with the exception of S1 A<sub>1</sub>P<sub>10</sub>, did not alter glial morphology in comparison to untreated controls as per GFAP staining (Figures 2D–2J). A DNA intercalating dye, DAPI, stained nuclei and pLuc in the cytoplasm. The cytoplasmic DNA staining indicated that polyplexes were in the cytoplasm (Figures 2E–2J). The cytoplasmic DAPI staining was most distinct in S1 A<sub>1</sub>P<sub>10</sub>-treated astrocytes (arrows in Figure 2E).

In neurons, S2 A<sub>5</sub>P<sub>10</sub> transfection led to the highest luciferase expression compared to all other polyplexes except S2 A<sub>1</sub>P<sub>10</sub> (\**p* < 0.05). Buffer pH or the proportion of arginine residues used during synthesis did not affect the transfection levels in human neurons (Figure 3A). In neurons, S1 A<sub>1</sub>P<sub>10</sub> was the most cytotoxic compared to the other polymers (\*\*\**p* < 0.001) as measured with LDH and MTT activities, respectively (Figures 3B and 3C). Except S1 A<sub>1</sub>P<sub>10</sub>, none of the polyplexes altered neuronal morphology compared to controls as characterized by microtubule associated protein 2 (MAP2) staining (Figures 3D and 3F–3J). However, S1 A<sub>1</sub>P<sub>10</sub>-treated neurons showed loss of processes and constricted cell bodies (arrows in Figure 3E). Co-staining with GFAP indicated a small number of astrocytes in the neuronal cultures, which were similar in all treatments.

Overall, S2 polymers led to higher luciferase activity and better biocompatibility compared to their S1 counterparts in both astrocytes and neurons. Therefore, only S2 polymers were used in the follow-up studies.

#### Time-Based Kinetics Reveals a Rapid Uptake of S2 Polyplexes and Sustained Gene Expression in Primary Human Astrocytes

To evaluate the uptake pattern of polyplexes in primary human astrocytes, two different transfection paradigms were implemented. In the first method, consistent with the previous experiments, cells were treated with polyplexes for 3 hr, then polyplexes were “washed” and fresh media was replenished (Figures 4A–4C). In the second paradigm, cells were left “unwashed” (Figures 4D–4F). Luciferase activity was measured at 3, 8, 24, and 48 hr post-transfection (Figures 4A and 4D). In both the treatment paradigms, luciferase expression was undetectable at 3 hr, detectable at 8 hr, and increased at 24 and 48 hr in A<sub>1</sub>P<sub>10</sub> (Figures 4A and 4D, red line, squares)- and A<sub>5</sub>P<sub>10</sub> (Figures 4A and 4D, blue line, triangles)-treated cells. A<sub>1</sub>P<sub>10</sub>- and A<sub>5</sub>P<sub>10</sub>-mediated luciferase expression was higher compared to A<sub>7</sub>P<sub>10</sub> (green line, inverted triangles) at 24 and 48 hr in both the paradigms (<sup>§</sup>*p* < 0.05) (Figures 4A and 4D). A<sub>1</sub>P<sub>10</sub>-facilitated protein expression in washed cells was also considerably higher than A<sub>5</sub>P<sub>10</sub> at 48 hr (<sup>#</sup>*p* < 0.05) (Figure 4A). Simultaneous cytotoxicity assays depicted no change in LDH activity in cells treated for 3 hr (Figure 4B), and it increased by 8%–15% at 48 hr in continuous treatment (\*\*\**p* < 0.001) (Figure 4E). The metabolic activity recovered in both the paradigms after an initial reduction at 8 hr (\*\**p* < 0.01) and was comparable to untreated controls (Figures 4C and 4F). Collectively,

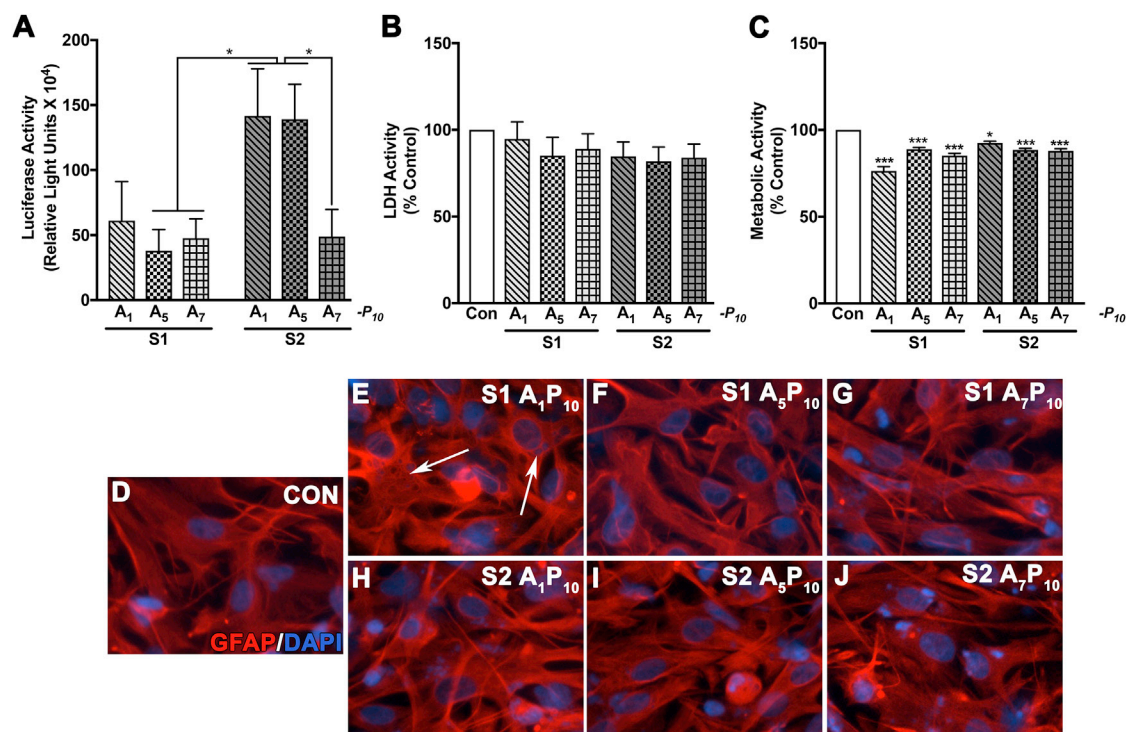


**Figure 2. The Transfection Levels and Biocompatibility of A<sub>n</sub>P<sub>n</sub> in Human Astrocytes are Affected by pH and Number of Arginine Residues**

Arginine-modified PEI polymer derivatives synthesized by method S1 or S2 containing 1, 5, or 7 arginine residues (A<sub>1</sub>, A<sub>5</sub>, A<sub>7</sub>) and 10 polyethylene glycol (PEG) (P<sub>10</sub>) residues/PEI molecule were mixed with pLuc in a 2:1 ratio. Human astrocytes (150,000/well) were treated with A<sub>n</sub>P<sub>n</sub> polyplexes. After 3 hr, polyplex containing-media was removed, and fresh culture medium was added. (A) Luciferase, (B) LDH, and (C) metabolic activities were measured 48 hr post-treatment. Data represent mean ± SEM for three donors with a minimum of triplicate determinations/donor (\*p < 0.05, \*\*\*p < 0.001). In parallel, astrocytes were immunostained for astrocyte-specific glial fibrillary acidic protein (GFAP; red) and nuclear dye DAPI (blue). (D) Untreated control, (E) S1 A<sub>1</sub>P<sub>10</sub>, (F) S1 A<sub>5</sub>P<sub>10</sub>, (G) S1 A<sub>7</sub>P<sub>10</sub>, (H) S2 A<sub>1</sub>P<sub>10</sub>, (I) S2 A<sub>5</sub>P<sub>10</sub>, and (J) S2 A<sub>7</sub>P<sub>10</sub>. Arrows indicate astrocytes with distinct cytoplasmic pDNA staining in endosomes. Representative donor images from four independent donors are shown. Original magnification ×200.

these results indicate that optimal polyplex uptake occurs in a few minutes to hours, while cytotoxicity assays demonstrate that polyplexes are biocompatible even following a prolonged exposure to cells.

After delineating the cellular uptake pattern, we evaluated the sustained luciferase expression obtained with S2 analogs. To delineate this, human astrocytes were treated with polyplexes for 3 hr, and luciferase expression was assessed at time points starting at 8 hr through 10 days (Figure 5A). Consistent with the previous data in Figure 4, luciferase activity was detectable at 8 hr and peaked at 2 days post-treatment. Expression dropped at 4 days (~75% from day 2) and then remained stable until 7 days. Both A<sub>1</sub>P<sub>10</sub> (Figure 5A, red line, squares) and A<sub>5</sub>P<sub>10</sub> (Figure 5A, blue line, triangles) consistently depicted higher expression compared to A<sub>7</sub>P<sub>10</sub> (Figure 5A, green line, inverted triangles) at 2 days, 4 days, and 7 days, respectively (<sup>sss</sup>p < 0.001). At 7 days, luciferase expression was higher in A<sub>1</sub>P<sub>10</sub> polyplex-treated cells than in A<sub>5</sub>P<sub>10</sub> polyplex-treated cells (<sup>###</sup>p < 0.001) (Figure 5A). Beyond 7 days, luciferase expression, while detectable, dropped inconsistently up to 10 days in astrocytes derived from multiple brain tissues (data not shown). In parallel, LDH and MTT activities were measured at 4 days and 10 days (Figures 5B and 5C).

LDH activity increased for A<sub>1</sub>P<sub>10</sub> and A<sub>5</sub>P<sub>10</sub> at 4 days (<sup>\*\*\*</sup>p < 0.001); however, it recovered and was comparable to untreated controls at 10 days (Figure 5B). Metabolic activity decreased in A<sub>7</sub>P<sub>10</sub>-polyplex treated cells at 4 days and in all treatments at 10 days (<sup>\*\*\*</sup>p < 0.001, ~11%–18%) (Figure 5C), which was comparable to the drop in metabolic activity seen at 2 days (Figure 2C).

Taken together, these results depict that cellular uptake of polyplexes with a short exposure can successfully sustain gene expression over longer time periods.

#### Polymer-mediated, GFAP-promoter-driven Gene Delivery to Human Astrocytes

Brenner and colleagues<sup>10,26</sup> have reported a 2.1-kb region of the GFAP promoter i.e., gfa2, and truncated portions of gfa2, i.e., gfa28 and gfaABC1D are responsible for restricting gene expression to either a specific brain region or to astrocytes. A luciferase reporter gene was sub-cloned downstream of these GFAP promoters (Figure 6A). Next, we tested delivery of GFAP promoter-driven luciferase plasmids using A<sub>n</sub>P<sub>n</sub>. Due to their highest transfection levels, we complexed A<sub>1</sub>P<sub>10</sub> and A<sub>5</sub>P<sub>10</sub> with each GFAP promoter construct

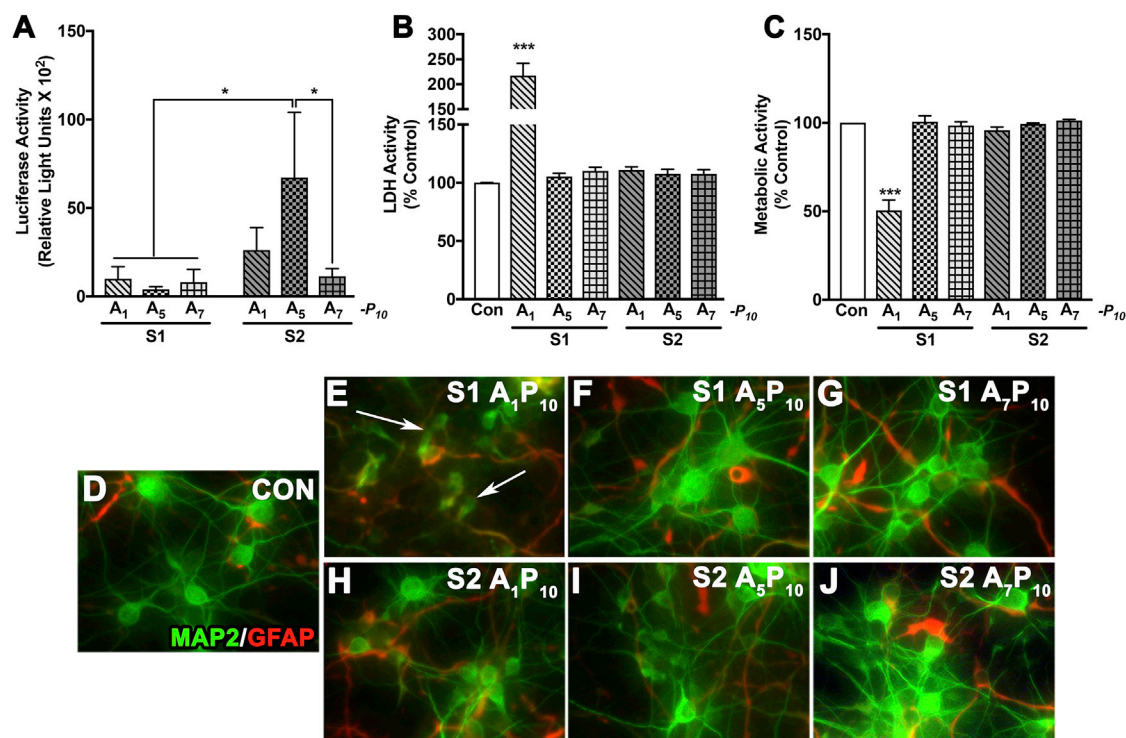


**Figure 3.  $A_nP_n$  Polyplexes Express Reporter Gene and Are Biocompatible in Primary Human Neurons**

Arginine-modified PEI polymer derivatives synthesized by method S1 or S2 containing 1, 5, or 7 arginine residues ( $A_1$ ,  $A_5$ ,  $A_7$ ) and 10 PEG ( $P_{10}$ ) residues/PEI molecule were mixed with pLuc in 2:1 w/w ratio. Human neurons (100,000/well) were treated with  $A_nP_n$  polyplexes for 3 hr. The polyplex containing-media was removed, and fresh culture medium was added. After 48 hr, (A) luciferase, (B) LDH, and (C) metabolic activities were measured. Data represent mean  $\pm$  SEM for three to five human donors with a minimum of triplicate determinations/donor ( $*p < 0.05$ ,  $***p < 0.001$ ). In parallel, neurons were immunostained for neuron-specific microtubule associated protein 2 (MAP2, green). GFAP (red) staining indicated presence of astrocytes in the neuronal cultures (D) untreated control, (E)  $S1 A_1P_{10}$ , (F)  $S1 A_5P_{10}$ , (G)  $S1 A_7P_{10}$ , (H)  $S2 A_1P_{10}$ , (I)  $S2 A_5P_{10}$ , and (J)  $S2 A_7P_{10}$ . Arrows indicate neurons without well-defined processes and shrunken cell bodies. Representative images from three individual donors are shown. Original magnification  $\times 200$ .

(gfa-Luc) at 2:1 w/w ratio. Astrocytes were treated with polyplexes for 3 hr, and luciferase levels were measured at 48 hr. While weak luciferase expression was measured in cells transfected with gfa2-Luc with both polyplexes, gfa28-Luc and gfaABC1D-Luc led to higher luciferase activity (Figure 6B). In  $A_1P_{10}$ -mediated transfections, gfaABC1D-driven gene expression was higher as compared to gfa2 ( $*p < 0.05$ ). In parallel,  $A_5P_{10}$ -mediated gfa28-Luc transfection resulted in higher expression compared to gfa2-luc ( $*p < 0.05$ ) (Figure 6B). Overall lower luciferase activity levels could be attributed to weaker GFAP promoter activity; however, these results highlight consistent transfection capabilities of polymers confirming their translational feasibility for astrocyte-targeted gene delivery.

#### Hemocompatibility of $A_nP_n$ Polyplexes and Polyplex-Mediated Gene Delivery to Mouse Brains

Prior to confirming delivery to mouse brains, it was critical to confirm the hemocompatibility of polyplexes. Human RBCs were isolated from healthy human donors and were incubated with polyplexes for 3 hr at room temperature (RT). Deionized water was used as a positive control. Lysis of RBCs incubated with all analogs, except S1

$A_1P_{10}$  and  $S2 A_7P_{10}$  was  $\geq 0.25\%$  or undetectable indicating good hemocompatibility (Figure 7A). With  $S2 A_7P_{10}$ , RBC lysis was marginally higher ( $\sim 2.2\%$ ). Significant RBC lysis was observed with  $S1 A_1P_{10}$  ( $\sim 5.5\%$ ) when compared to the negative control (1X PBS). Additionally, none of the polyplexes induced RBC aggregation (data not shown).

After confirming hemocompatibility in human RBCs, we wanted to validate *in vivo* polymer-mediated i.v. gene delivery. For this,  $S2 A_5P_{10}$ -pLuc polyplexes were injected via tail vein to athymic nude (nu/nu) mice. Luciferase expression was evaluated in the liver and brain tissues (Figure 7B) at 24, 48, and 72 hr following three injections. Liver tissue isolates depicted little to no luciferase expression compared to baseline controls. For brain isolates, the highest luciferase activity was measured at 48 hr, while brains isolated at 24 hr and 72 hr showed marginally higher luciferase activity than the control brain isolates. Immunohistochemical analyses were performed to detect luciferase localization in the mice brains. Confocal micrographs showed luciferase expression in the cortical brain regions in astrocytes (arrowheads in Figures 7D4 and 7E4) as well as

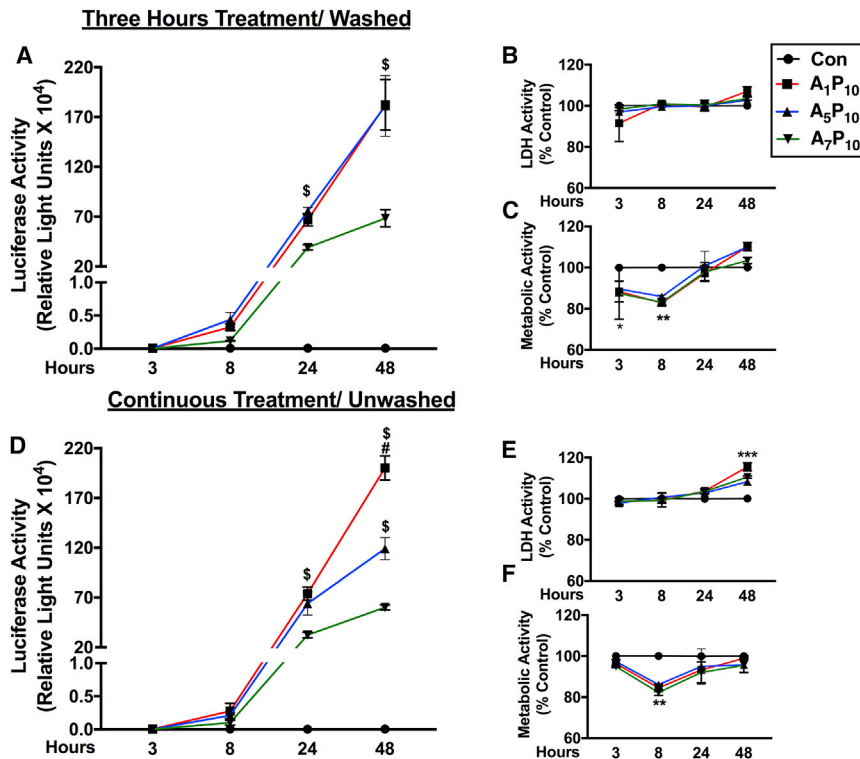


**Figure 4. Polyplex Exposure Duration Does Not Contribute to Efficacy of Gene Expression and Biocompatibility in Astrocytes**

Human astrocytes (150,000/well) were treated with S2 polymer:pDNA polyplexes (A–C) for 3 hr and washed or (D–F) left unwashed prior to testing. (A and D) Luciferase activity, (B and E) LDH activity, and (C and F) metabolic activity was measured at 3, 8, 24, and 48 hr post-treatment (A<sub>7</sub>P<sub>10</sub> red line, A<sub>5</sub>P<sub>10</sub> blue line, A<sub>7</sub>P<sub>10</sub> green line). Data represent mean ± SEM for two donors with a minimum of triplicate determinations/donor (\*p < 0.05 for comparison to A<sub>7</sub>P<sub>10</sub>; #p < 0.05 for comparison to A<sub>5</sub>P<sub>10</sub>, \*p < 0.05, \*\*p < 0.01, \*\*\*p < 0.001 versus controls at a specific time point).

diverse morphologies and distinct electrophysiological properties as compared to rodent astrocytes.<sup>32,33</sup> Furthermore, gene-expression profiles of human and rodent astrocytes are markedly different.<sup>34</sup> These findings suggest that the source species of astrocytes could impact their ability to express a gene or functional effects of therapeutic gene expression. Few viral vector-based studies have also highlighted species of tested animals to be a critical aspect in determining cell-type-specific gene-expression patterns.<sup>24,25</sup> In this context,

primary neural cells from over a dozen independent human tissues were used in our study. To our knowledge, this is the first proof-of-concept study simultaneously depicting polymer-mediated gene delivery to primary human brain cells and capable of traversing the BBB in rodent models.

Polyplex-based transfections are influenced by several factors, including DNA condensation, cellular uptake, cytoplasmic delivery, and DNA release from polyplexes for nuclear localization. Important factors also include stability and aggregation in the presence of serum proteins, biocompatibility, and hemocompatibility. The presented study addressed each of these aspects by implementing stepwise, deliberate investigations to depict successful gene delivery to primary neural cells. First, we determined that the optimal polyplex ratio, which would condense pDNA, would not affect plasma membrane interactions and facilitate their endosomal escape. A 2:1 w/w ratio was found to be more suitable than other combinations with respect to transfection levels and biocompatibility (Figure 1). The gel electrophoresis data also show DNA condensation at this ratio (data not shown). More importantly, the higher viability of A<sub>n</sub>P<sub>n</sub>-transfected cells compared to PEI transfections indicated that the PEG modifications reduced PEI toxicity, while maintaining the same or higher transfection levels (Figures 1A and 1C).

Changes in pH may rearrange polymer components, ultimately affecting its DNA binding and delivery efficiency. To analyze pH-associated changes, MES and PBS buffer pH was not adjusted (S1)

other cells as indicated by luciferase-GFAP co-staining (Figures 7D, Con; 7E, 24 hr; and 7F, 48 hr). We anticipate that using constructs with GFAP promoters will restrict the expression to astrocytes and eliminate off-target effects. In summary, polyplexes effectively crossed the BBB and delivered pDNA to brain cells, which underscores a broader gene-delivery potential of our polyplex-based gene delivery system.

## DISCUSSION

In the past few years, CNS-targeted therapeutics have been in great need, owing to increasing global prevalence of NDDs and lack of effective treatment options. Astrocytes have emerged as critical functional components of the CNS. Our review of the current literature<sup>1</sup> suggested that astrocyte-directed CNS therapies are pre-destined in the near future. This study is a first step in that direction, testing a gene-therapy approach using biocompatible and hemocompatible polyplexes that demonstrated cellular uptake and sustained gene expression in primary neural cells and *in vivo* in mice.

Selecting the appropriate *in vitro* model is a critical first step for evaluating translational potential of human therapies. Prior studies have successfully targeted astrocytes using viral or non-viral gene-delivery systems in rodent disease models including for neuropathic pain<sup>27</sup> and in Alzheimer's disease,<sup>28</sup> Parkinson's disease,<sup>29</sup> and Huntington's disease.<sup>30,31</sup> Results from these studies validate the utility of targeting astrocytes for CNS therapeutics. However, human astrocytes have

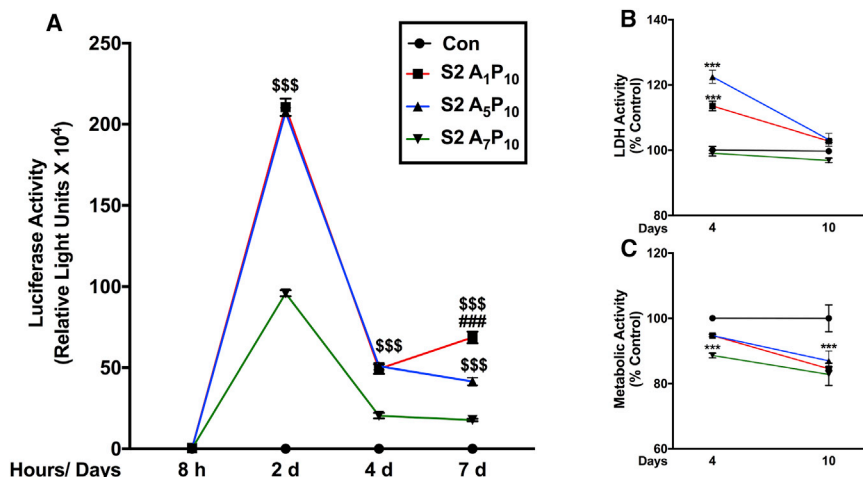


**Figure 5. Polyplex-mediated Gene Expression Is Sustained for Over a Week in Primary Human Astrocytes**

Human astrocytes (150,000/well) were treated with S2 polymer:pDNA polyplexes for 3 hr and washed. (A) Luciferase activity was measured at 8 hr (h), 2 days (d), 4 days, and 7 days post-treatment. (B) LDH and (C) metabolic activities were measured 4 days and 10 days post-treatment (A<sub>1</sub>P<sub>10</sub> red line, A<sub>5</sub>P<sub>10</sub> blue line, A<sub>7</sub>P<sub>10</sub> green line). Data represent mean  $\pm$  SEM for representative donor from five donors with a minimum of triplicate determinations/donor (<sup>\$\$\$</sup>p < 0.001 for A<sub>1</sub>P<sub>10</sub> and A<sub>5</sub>P<sub>10</sub> versus A<sub>7</sub>P<sub>10</sub>; <sup>###</sup>p < 0.001, A<sub>1</sub>P<sub>10</sub> versus A<sub>5</sub>P<sub>10</sub>, <sup>\*\*\*</sup>p < 0.001 versus controls; at a specific time point).

or pre-adjusted (S2). The physicochemical characteristics of all the polymers were comparable, and no specific changes were observed in the context of the buffer pH adjustments (Table 1). However, both astrocytes and neurons transfected with S2 polymers showed overall higher luciferase expression, indicating increased transfection (Figures 2A and 3A). The difference in luciferase expression with S1 and S2 polymers could be due to effects of altered buffer pH on arginine, PEG, and PEI conjugation efficiency in the overall composition. Alternately, the reactants in the S2 formulation could have formed stable structures, owing to higher conjugation efficacy at the pre-adjusted buffer pH, leading to higher transfection. Further investigations are necessary to delineate the underlying physicochemical changes, which could influence transfection levels. Nonetheless, luciferase activity observed with all polyplexes established their utility in transfection studies.

Some aspects of intracellular gene delivery mechanisms of PEI have been well demonstrated. First, endocytic vesicles internalize PEI-based polyplexes. Highly protonable amines of PEI bind H<sup>+</sup> ions reduce pH and destabilize lysosomal enzymes, causing osmotic swelling and subsequent endosomal escape of polyplexes by vacuole disruption.<sup>35,36</sup> Further mechanisms of cytoplasmic release and nuclear membrane crossing of pDNA are unclear.<sup>37</sup> We observed luciferase expression at 8 hr, indicating the nuclear entry of pDNA and subsequent transcription and translation within that time frame post-transfection. However, gene expression kinetics were not well understood. Therefore, cellular uptake and sustained gene expression of A<sub>n</sub>P<sub>n</sub> polyplexes were evaluated. It was observed that uptake occurred with a short exposure of a few minutes to hours, and expression was sustained for over a week in primary astrocyte cultures without cytotoxicity (Figures 4 and 5). It is unclear if there is a retrograde polyplex release and reuptake by cells from the culture media or if the polyplexes persist in cytoplasm without being metabolized and release pDNA over time. Regardless of the mechanism, these results are promising since this non-viral delivery system can be used in disease models where a transient, yet stable gene expression is required without the risk of genomic DNA integration observed

with viral vectors. It must be noted that our *in vivo* experiments did not indicate a sustained expression pattern (Figure 7B), and these studies are in incipient stages and thorough investigations are warranted to delineate the *in vivo* expression kinetics.

It has been shown previously that PEI or its derivatives mediate *in vitro* or *in vivo* neuronal gene delivery in rats,<sup>38</sup> mice,<sup>15</sup> or brain-derived primary cells and cancer cell lines.<sup>39,40</sup> We also showed A<sub>n</sub>P<sub>n</sub>-mediated luciferase expression in primary neuronal cultures (Figure 3A); however, our objective was to validate a gene-delivery system capable of astrocyte targeting. Hence, neuronal A<sub>n</sub>P<sub>n</sub> polyplex treatments were predominantly focused on ruling out an off-target neuronal cytotoxicity (Figures 3B and 3C). Concurrent luciferase activity in neuronal cultures was approximately 1,000-fold lower than astrocytes (Figures 2A and 3A). This could be due to cell culture conditions, which are strikingly different for neurons versus astrocytes. Primary human neurons were cultured in serum-free medium to restrict the growth of astrocytes after isolation from human brain tissues. We obtained over 90%–95% neuronal purity with a small number of astrocytes in cultures based on MAP2 and GFAP staining (Figures 3D–3J). It is unclear if the luciferase activity seen in these cultures is coming from neurons or astrocytes. The polyplexes may possess an intrinsic glial tropism leading to more polyplex molecules binding to astrocytes, resulting in higher transfection levels. Alternately, astrocytes may take up the polyplexes more efficiently during proliferating phase in culture, which could subsequently increase gene expression compared to terminally differentiated neurons (Figures 2A and 3A). Though the underlying mechanisms are not well understood at this time, these results are encouraging from a glia-targeting perspective.

A more direct approach to restrict off-target effects of gene delivery is to use a promoter restricted to a specific target cell type. The gfa2 segment in the 5' region of the GFAP promoter was identified to be capable of restricting gene expression to astrocytes.<sup>26</sup> Since then, the gfa2 promoter has been used in astrocyte targeting studies,<sup>28,41</sup> in transgenic rodent models,<sup>42</sup> and to study astrocyte function.<sup>31,43</sup>

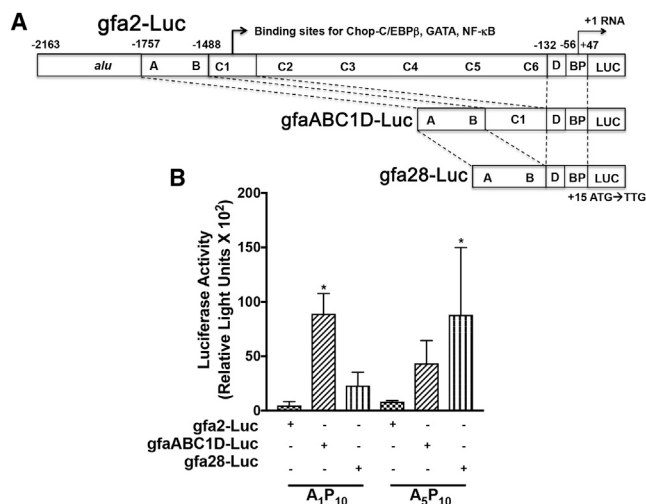


**Figure 6. Select S2 Polymers Successfully Deliver GFAP Promoter Fragment Driven-Luciferase Expression in Human Astrocytes**

(A) Plasmids with GFAP promoter segments (gfa2, gfa28, and gfaABC1D) were used to drive luciferase (Luc). These promoter regions have been reported to restrict gene expression to a region and/or astrocytes in the brain. (B) Human astrocytes (150,000/well) were transfected with select S2 A<sub>1</sub>P<sub>10</sub> and A<sub>5</sub>P<sub>10</sub>;pgfa-Luc plasmids for 3 hr and washed. Luciferase activity was measured 48 hr post-treatment. Data represents mean  $\pm$  SEM for two donors with a minimum of triplicate determinations/donor (\**p* < 0.05 versus gfa2-Luc for the same polyplex).

Subsequent experiments showed that segments within gfa2, namely gfa28, restrict gene expression to a specific brain region, and gfaABC1D restricts it to astrocytes throughout the brain<sup>10</sup> (Figure 6A). We successfully used S2 A<sub>1</sub>P<sub>10</sub> and S2 A<sub>5</sub>P<sub>10</sub> to transfect astrocytes with GFAP promoter-driven constructs (Figure 6B). The gfa28 promoter is not specific to astrocytes, restricting expression to dorsal and caudal cortical regions, hippocampus, and caudal vermis of the cerebellum.<sup>44</sup> On the other hand, the gfaABC1D promoter expresses ubiquitously through the brain and is restricted to astrocytes.<sup>10</sup> These differences in expression patterns can be used in targeting astrocytes for specific disease conditions, e.g., a gfa28 promoter may not be used for designing therapeutics for Parkinson's disease, in which the substantia nigra located in the midbrain is the primary affected area;<sup>14</sup> however, it can be used for treating HIV-associated neurocognitive disorders, in which white matter loss in the corpus callosum region is observed.<sup>45</sup> It must be noted that GFAP is a weak promoter compared to viral cytomegalovirus (CMV) and simian virus 40 (SV40) promoters. Thus, additional manipulations of the promoter sequence, such as upstream insertion of a CMV enhancer or inverted terminal repeats,<sup>46</sup> may obtain substantial gene expression.

For CNS-targeted therapies, a significant obstacle exists in the form of the BBB. In our studies, S2 A<sub>5</sub>P<sub>10</sub> successfully crossed the BBB, and reporter expression was detected in the brain after i.v. tail-vein injection in mice (Figures 7B and 7C). It was surprising that there was little to no luciferase expression detected in the liver at any tested time points. Nonetheless, these results are consistent with previous findings that investigated gene delivery with PEI derivatives.<sup>47,48</sup>

We speculate that in the liver either the polyplexes get metabolized rapidly prior to pDNA release or may be excreted from liver via biliary duct to the gut. Alternately, luciferase could be metabolized immediately post-translation in hepatocytes. Brain-targeted gene therapies have adopted other methods to circumvent or facilitate entry through the BBB, such as intrastriatal<sup>49</sup> or ventricular injections<sup>50</sup> and focused ultrasound.<sup>51</sup> Considering the invasiveness or complexity of these methods, i.v. delivery is preferable.

Viral vectors have thrived and transitioned better in pre-clinical brain-targeted gene delivery studies, and all current gene therapy clinical trials for NDDs use viral vectors.<sup>52</sup> Some of these studies have reported issues, such as immunogenicity and lack of efficacy in early-phase clinical trials.<sup>14,53</sup> In comparison, investigations testing non-viral gene delivery for NDDs have been fickle due to lack of biocompatibility, efficacy, and inability to cross the BBB. Our study is well timed in this aspect, as we address the unmet need of a biocompatible and effective gene-delivery system.

## Conclusions

While neurons are the ultimate therapeutic cellular destination for treating neurodegeneration, reaching the "stars," i.e., astrocytes, first will be more practical and effective. Gene delivery systems, including viral vectors, inorganic nanoparticles, and lipomers are being tested for targeting gene therapy to the brain. Each of these systems has its own set of shortcomings that include but are not limited to immunogenicity, toxicity, and inadequate efficacy. Our current study convincingly shows that we have a non-viral, biocompatible, and effective delivery system for targeting gene therapy to primary human neural cells and mouse brains. We propose that this approach will provide a powerful tool for delivering therapeutic genes not only to the brain, but also other difficult cell targets.

## MATERIALS AND METHODS

### Synthesis of A<sub>n</sub>P<sub>n</sub> Polymers

3-(2-aminoethylamino) propyl-methyl-dimethoxysilane was purchased from Fluka (Sigma-Aldrich, St. Louis, MO). PEI, branched, molecular weight (MW) 25 kDa; N-hydroxysuccinimide (NHS); PEG bis(carboxymethyl)ether, MW 600 Da (PEG); 1-ethyl-3-(3-dimethylaminopropyl)carbodiimide hydrochloride (EDC); N $\alpha$ -(tert-butoxycarbonyl)-aspartic acid (Boc-Asp); 2-(N-morpholino) ethanesulfonic acid (MES); and L-arginine were purchased from Sigma-Aldrich (St. Louis, MO).

Oligo-(alkylaminosiloxane) was prepared as described previously.<sup>54</sup> In brief, 1 eq of 1 N NaOH solution (32  $\mu$ L) was added to 1.8 mmol (0.371 g, 1 eq) of 3-(2-aminoethylamino) propyl-methyl-dimethoxysilane and stirred for 20 hr at RT. The removal of residual solvent and small volatiles gives oligo-(alkylaminosiloxane). The schematic of this reaction and resulting polymer compositions have been described previously.<sup>55</sup>

Next, L-arginine, PEI, and PEG were conjugated in consecutive steps onto oligo-(alkylaminosiloxane) by a four-step reaction using



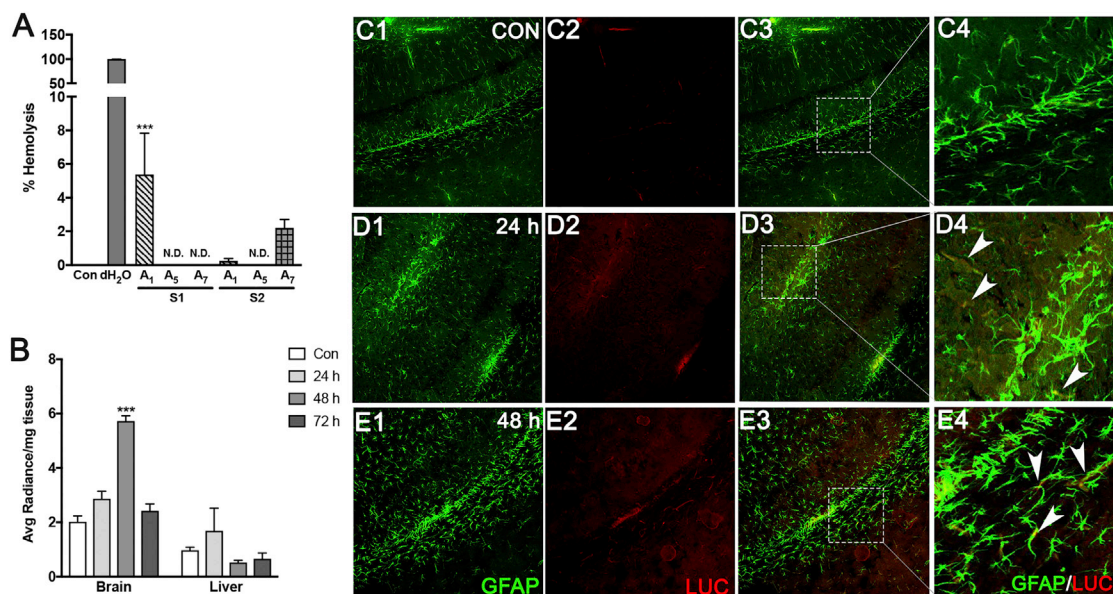


**Figure 7. Polyplexes Induce Little to No Hemolysis and Mediate Reporter Gene Expression in Mouse Brains**

(A) Whole human blood was centrifuged at 2,000 rpm. Pelleted red blood cells were mixed in saline at a 1:6 ratio and incubated at 37°C with polyplexes (2:1 w/w ratio) for 3 hr. PBS (1X) and deionized water were used as negative and positive controls, respectively. Post-incubation, supernatants were analyzed to measure % hemolysis compared to controls. Data shown represent mean ± SEM from three donors with a minimum of triplicate determinations/donor (\*\*p < 0.01, \*\*\*p < 0.001). (B) Athymic nude mice were injected intravenously with S2 A<sub>6</sub>P<sub>10</sub>:pLuc polyplexes (100 μg polymer and 50 μg pDNA/dose) for 3 days. Brains and livers were cut into small pieces and incubated with *in vivo* glo-d-luciferin in well plates. Luciferase activity was assessed in tissue isolates harvested at 24, 48, and 72 hr after last injection. Data shown represent mean ± SEM for 3 to 4 mice per condition (\*\*p < 0.01, \*\*\*p < 0.001). (C1–E4) In a parallel experiment, brains harvested at 24 and 48 hr were fixed with 4% paraformaldehyde, and 40 μM frozen coronal sections were cut immunostained for GFAP (green) and luc (red). (C) Control, (D) 24 hr, (E) 48 hr. Arrowheads represent cells co-stained for luciferase and GFAP. n = 3 or 4 mice per condition. Each image was captured as 8–15 Z sections using a confocal microscope. Representative images from the cortical regions of brain are shown. Original magnification ×100.

1-ethyl-3-(3-dimethylaminopropyl)carbodiimide chemistry.<sup>23</sup> For every conjugation reaction, carboxylic acid activation and the reaction between amine and activated carboxylic acid were carried out in MES and PBS buffer, respectively. Two types of polymers were synthesized. The first type were synthesized by not adjusting the pH (S1) and the second type by adjusting the pH of MES (6.5) and PBS (7.2) buffers, using HCl and NaOH after adding all the reactants (S2). The conjugation efficiency is expected to be higher when the activation of carboxylic acid is performed at pH 6.5, and the reaction between activated carboxylic acid and amine is performed at pH 7.2. All polymers were dialyzed extensively against milli Q water to remove untreated monomers and freeze-dried.

#### Plasmids, Sub-cloning, and Amplification

All gene delivery experiments were carried out using cytomegalovirus promoter-driven luciferase as a reporter plasmid vector unless specified otherwise. Reporter pLuc was amplified by transforming *Escherichia coli* DH5α competent cells and isolated using endotoxin-free pDNA isolation kits according to manufacturer's instructions (QIAGEN, Valencia, CA). All GFAP promoter-encoding constructs gfa2-lacZ (catalog no. 53126), gfa28-LacZ (catalog no. 53130), and gfaABC1D-LacZ (catalog no. 53131) were obtained from Addgene (courtesy of Dr. Michael Brenner).<sup>10,26</sup> Sub-cloning was carried out using restriction digest, followed by DNA ligation.

All reagents were purchased from New England Biolabs (Ipswich, MA) unless otherwise specified. Luciferase open reading frame (ORF) was excised from pLuc by restriction digestion using Nco-I (catalog no. R0193) and Xba-I (catalog no. R0145). The GFAP promoter constructs were digested with Nco-I and NgoMIV (catalog no. R0564) to remove LacZ ORF. Restriction digests were run on an agarose gel, and a DNA gel extraction kit was used to isolate required fragments (QIAGEN, Valencia, CA). Short oligonucleotide sequences were ordered from Sigma (St. Louis, MO). The oligos were designed such that two oligo strands formed double-stranded DNA inserts with 5' sticky ends for Xba-I and NgoMIV. Equimolar concentrations of complementary oligonucleotides were mixed and incubated at 85°C for 5 min and cooled down to RT. The fragments (luciferase ORF, GFAP promoter plasmids without LacZ ORF, double-stranded oligos) were mixed with DNA ligase as per manufacturer's instructions. Subsequently, DH5α competent cells were transformed with ligated products. Appropriately ligated clones were obtained after a series of plasmid minipreps and restriction digests, which were then isolated using endotoxin-free pDNA isolation kits (QIAGEN, Valencia, CA).

#### Characterization of A<sub>n</sub>P<sub>n</sub>: pDNA Polyplexes

Polymers and pDNA were dissolved in nuclease-free water at a concentration of 1 mg/mL. Polyplexes were prepared in 5 mM PBS

(pH 7.4) by mixing pDNA with different amounts of polymer and medium. The pDNA-polymer solutions were mixed well by triturating, vortexed, and then incubated for 15–20 min at RT. Polyplex size and zeta potential were determined using quasi-elastic light scattering (PSS/NICOMP 380/ZLS Particle Sizing Systems, Santa Barbara, CA).

### Cell Culture

Primary human astrocytes and neurons were harvested from first- and early second-trimester fetal specimens, obtained from the Birth Defects Research Laboratory, University of Washington (Seattle, WA), in full compliance with the ethical guidelines of the NIH (Bethesda, MD), University of Washington, and University of North Texas Health Science Center (Fort Worth, TX). The Birth Defects Research Laboratory obtained written consent from all tissue donors. Human neurons and astrocytes were isolated as previously described.<sup>56</sup> Human neurons were cultured on poly-d-lysine-treated plates in neurobasal medium with  $1 \times$  B27 supplement for 2–4 weeks before treatments. Astrocytes were cultured in 1:1 v/v DMEM:F12 medium with 10% fetal bovine serum (Peak Serum, lot no. 17C161) for 20–24 hr before treatments. Both media contained  $1 \times$  penicillin-streptomycin-neomycin (PSN) (catalog no. P4083, Sigma Aldrich, St. Louis, MO) and Fungizone (catalog no. A9528, Sigma Aldrich, St. Louis, MO). Neurons were plated at a density of 100,000 cells/well and astrocytes at 150,000 cells/well in 48-well plates. All reagents for cell culture media were Gibco brand (Fisher Scientific, Waltham, MA) unless otherwise specified.

### Transfecting with Polyplexes *In Vitro*

All transfection experiments were carried out with cells cultured in 48-well plates. Polymers and pDNA were dissolved in culture medium at a concentration of 1 mg/mL. The polyplexes were prepared by mixing appropriate amounts of pDNA and polymer in culture media to make a final volume of 15  $\mu$ L/well. The mixtures were incubated for 15–20 min at RT for polyplex formation. More culture medium was added to the polyplexes before adding to cells and final concentration of the pDNA in each well was 1  $\mu$ g/well. Unless otherwise specified, cells were treated with polymer:pDNA for 3 hr, polyplexes were then “washed” after 3 hr, fresh culture medium was added, and end-point assays were carried out 48 hr post-treatment. For  $A_nP_n$ -pDNA uptake experiments, an additional treatment paradigm was used in which cells were left “unwashed” at 3 hr, and media was not replaced prior to protein expression and cytotoxicity evaluations.

### Determination of Luciferase Activity *In Vitro*

The culture media was removed from wells and cells were lysed with 65  $\mu$ L of  $1 \times$  reporter lysis buffer. Then, lysates were loaded in 96-well white-colored plates (20  $\mu$ L/well) and luciferase activity was measured according to manufacturer’s instructions (Promega, Madison, WI).

### Determination of Cytotoxicity

Metabolic activity of neural cells was measured by MTT assay as described previously.<sup>57</sup> Absorbance was measured at 490 nm using

a microplate reader (Molecular Devices, Sunnyvale, CA). Cell supernatants were collected and LDH activity was evaluated using a Cytotoxicity Detection Kit<sup>PLUS</sup> according to manufacturer’s instructions (Sigma Aldrich, St. Louis, MO). Cell lysates were collected, and DNA fragmentation was assessed by Cell Death Detection ELISA<sup>PLUS</sup> kit according to manufacturer’s protocol (Sigma Aldrich, St. Louis, MO).

### Evaluation of Hemocompatibility

RBC lysis in the presence of polyplexes was evaluated to determine their hemocompatibility. Blood was collected from healthy human volunteers in tubes containing potassium EDTA (Sigma-Aldrich). Collected whole blood was centrifuged at  $1,500 \times g$  for 10 min at RT (Sorvall Legend RT; Thermo Scientific, Waltham, MA), and RBCs were washed three times with PBS. To determine hemolysis, RBCs were diluted six times with PBS and incubated at RT with polyplexes (polymer:pDNA ratio 2:1 w/w) for 3 hr. The RBC-polyplex mixture was centrifuged for 10 min, and the supernatant (50  $\mu$ L) was dissolved in 150  $\mu$ L of 40:1 (v/v) ethanol: HCl mixture in a Nunc 96-well polypropylene MicroWell plate (Thermo Scientific, Waltham, MA). The absorbance was measured at 399 nm. RBCs incubated with deionized water were used as the positive control for complete lysis, and RBCs incubated with PBS served as no lysis control.

### Animals and *In Vivo* Transfection

Male, athymic nude (nu/nu) mice (5–6 weeks old) were purchased (Envigo, Allison Pointe Blvd, IN), housed in a temperature- and light-controlled room on a 12:12 hr light: dark cycle with *ad libitum* water and food. Cleveland Clinic’s institutional animal care and use committee approved all animal procedures, and these were carried out according to federal and internal guidelines. Mice were anesthetized with 2% isoflurane in oxygen and maintained in anaesthetized state during tail-vein injections using 1% isoflurane in oxygen via nose cone. Polyplexes containing 50  $\mu$ g of pDNA (2:1 w/w  $A_nP_n$ :pDNA) in 300  $\mu$ L saline were injected via tail vein on 3 consecutive days at 24-hr intervals. Animals not injected with polyplexes or DNA were used as controls to check for the background signal. At 24, 48, and 72 hr following the last injection, mice were anaesthetized and perfused with normal saline following cardiac puncture to wash out blood. Brains and livers were collected to determine the extent of protein expression. All organs following dissection were rinsed with saline, cut into small pieces, incubated with VivoGlo Luciferin (Promega) (1.5  $\mu$ g per 5 mg tissue weight) for 40 min in 24-well plates (Becton Dickinson Labware, Franklin Lakes, NJ) and imaged with IVIS Lumina II (PerkinElmer, Hopkinton, MA). The bioluminescence signal intensity (photons per square centimeter steradian [ $p/s/cm^2/sr$ ]) of the organs from the injected and uninjected mice were plotted. Each treatment group consisted of three to four mice and cumulative data has been shown.

### Immunocytochemistry and Immunohistochemistry

For immunocytochemistry, neural cells were fixed in acetone:methanol (1:1) for 15–20 min at  $-20^\circ\text{C}$ . After 30 min incubation

with blocking buffer, the cells were probed with primary antibodies and incubated overnight at 4°C. Human astrocytes were probed with primary antibody against GFAP (produced in rabbit, 1:700, catalog no. Z0334; Dako, Carpinteria, CA), and neuroglial cultures were probed with antibodies against MAP2 (produced in chicken, 1:2,000, catalogue no. Ab5392; Abcam, Cambridge, UK), and GFAP (produced in rabbit, 1:1,000; Dako, Carpinteria, CA). Then cells were washed three times in PBS and labeled according to primary antibodies with anti-chicken and/or rabbit (488 nm, green, or 594 nm, red) Alexa Fluor secondary antibodies (1:100, Thermo Fisher Scientific, Waltham, MA), for 1.5 hr at RT. Further, cells were washed thrice with PBS, and DAPI was added for 3 min at RT to visualize nuclei (1:1,000, blue, Thermo Fisher Scientific, Waltham, MA). Post-DAPI staining, images were taken at 100–200× magnification on Nikon Eclipse and processed by NIS-Element BR 3.2 software (Nikon, Melville, NY).

For immunohistochemical analysis, brains were harvested after perfusion of animals with saline. The brains were then fixed by immersing them into with 5 mL of 4% paraformaldehyde (Electron Microscopy Sciences, Hatfield, PA) diluted in 1× PBS. The harvested brains were cryopreserved in a 30% sucrose (Sigma-Aldrich) solution in 1× PBS at 4°C overnight. The brains were then frozen in the cryotome cryostat using Tissue-Tek-embedding medium (Sakura Finetek USA, Torrance, CA) at –20°C. Frozen coronal sections of the brain of 40-µm thickness were cut (CM 1900, Leica, Buffalo Grove, IL). After blocking (3% horse serum, 0.3% Triton X-100 in 1× PBS), sections were incubated at 4°C overnight with anti-luciferase antibody (produced in rabbit, 1:500, Abcam, Cambridge, UK) and GFAP antibody (produced in chicken, 1:1,000, catalog no. Poly28294, San Diego, CA). After washing the brain sections with PBS, they were stained appropriately with anti-chicken (488 nm, green) and -rabbit (488 nm, green) Alexa Fluor secondary antibodies (1:1,000). Finally, nuclear staining was done with DAPI. Images were taken at 100× magnification on Zeiss LSM 510 (Carl Zeiss AG, Oberkochen, Germany).

### Statistical Analyses

All numerical data were taken as mean ± SEM for analyses and statistical analysis was performed using GraphPad Prism 7.0. In cytotoxicity analyses, data were normalized with untreated controls, and raw data were used in luciferase assay analysis. All data were analyzed using a one-way (cytotoxicity assays) or a two-way ANOVA (luciferase assays) with Tukey or Fisher's least significant difference post-hoc tests for pairwise comparisons. Differences were considered statistically significant with  $p \leq 0.05$ .

### AUTHOR CONTRIBUTIONS

C.R.J. planned and conducted all the *in vitro* work and immunohistochemistry on mouse tissues, analyzed and interpreted the data, and wrote the manuscript. V.R. designed and optimized the synthesis of polymers. S.V. and Y.G. planned and conducted all *in vivo* experiments, data analysis, and interpretation. M.S. characterized polyplexes. V.L. advised on the polymer synthesis and experimental

design of the project, interpreted the data, and edited the manuscript. A.G. conceived and supervised the project, interpreted the data, and wrote the manuscript. All authors approved the final version of the manuscript.

### CONFLICTS OF INTEREST

The authors declare no conflict of interest.

### ACKNOWLEDGMENTS

The authors thank members of the Ghorpade laboratory at UNT Health Science Center and the Labhasetwar laboratory at Cleveland Clinic for their help with proofreading and critical reading of the manuscript. We appreciate the assistance of Laboratory of Developmental Biology for providing human brain tissues; also supported by NIH award number 5R24HD0008836 from the Eunice Kennedy Shriver National Institute of Child Health and Human Development. The authors would also like to acknowledge Ms. Lin Tang and Ms. Satomi Stacy at the Ghorpade laboratory for culturing and maintaining high-quality primary neural cells. The authors appreciate Ms. I-Fen Chang's help with confocal imaging of brain slices. The National Institute of Neurological Disorders and Stroke award R01 NS048837 to A.G. supported the presented work.

### REFERENCES

- Joshi, C.R., Labhasetwar, V., and Ghorpade, A. (2017). Destination Brain: the Past, Present, and Future of Therapeutic Gene Delivery. *J. Neuroimmune Pharmacol.* 12, 51–83.
- Barres, B.A. (2008). The mystery and magic of glia: a perspective on their roles in health and disease. *Neuron* 60, 430–440.
- Halassa, M.M., Fellin, T., and Haydon, P.G. (2007). The tripartite synapse: roles for gliotransmission in health and disease. *Trends Mol. Med.* 13, 54–63.
- Hamby, M.E., and Sofroniew, M.V. (2010). Reactive astrocytes as therapeutic targets for CNS disorders. *Neurotherapeutics* 7, 494–506.
- Cabezas, R., Avila-Rodriguez, M., Vega-Vela, N.E., Echeverria, V., González, J., Hidalgo, O.A., Santos, A.B., Aliev, G., and Barreto, G.E. (2016). Growth factors and astrocytes metabolism: Possible roles for platelet derived growth factor. *Med. Chem.* 12, 204–210.
- Gardner, J., and Ghorpade, A. (2003). Tissue inhibitor of metalloproteinase (TIMP)-1: the TIMPed balance of matrix metalloproteinases in the central nervous system. *J. Neurosci. Res.* 74, 801–806.
- Kiyota, T., Yamamoto, M., Schroder, B., Jacobsen, M.T., Swan, R.J., Lambert, M.P., Klein, W.L., Gendelman, H.E., Ransohoff, R.M., and Ikezu, T. (2009). AAV1/2-mediated CNS gene delivery of dominant-negative CCL2 mutant suppresses gliosis, β-amyloidosis, and learning impairment of APP/PS1 mice. *Mol. Ther.* 17, 803–809.
- Zheng, J.C., Huang, Y., Tang, K., Cui, M., Niemann, D., Lopez, A., Morgello, S., and Chen, S. (2008). HIV-1-infected and/or immune-activated macrophages regulate astrocyte CXCL8 production through IL-1β and TNF-α: involvement of mitogen-activated protein kinases and protein kinase R. *J. Neuroimmunol.* 200, 100–110.
- Niranjani, R. (2014). The role of inflammatory and oxidative stress mechanisms in the pathogenesis of Parkinson's disease: focus on astrocytes. *Mol. Neurobiol.* 49, 28–38.
- Lee, Y., Messing, A., Su, M., and Brenner, M. (2008). GFAP promoter elements required for region-specific and astrocyte-specific expression. *Glia* 56, 481–493.
- Regan, M.R., Huang, Y.H., Kim, Y.S., Dykes-Hoberg, M.L., Jin, L., Watkins, A.M., Bergles, D.E., and Rothstein, J.D. (2007). Variations in promoter activity reveal a differential expression and physiology of glutamate transporters by glia in the developing and mature CNS. *J. Neurosci.* 27, 6607–6619.

12. Adam, S.A., Schnell, O., Pöschl, J., Eigenbrod, S., Kretschmar, H.A., Tonn, J.C., and Schüller, U. (2012). ALDH1A1 is a marker of astrocytic differentiation during brain development and correlates with better survival in glioblastoma patients. *Brain Pathol.* *22*, 788–797.
13. Rafii, M.S., Baumann, T.L., Bakay, R.A., Ostrove, J.M., Siffert, J., Fleisher, A.S., Herzog, C.D., Barba, D., Pay, M., Salmon, D.P., et al. (2014). A phase I study of stereotactic gene delivery of AAV2-NGF for Alzheimer's disease. *Alzheimers Dement.* *10*, 571–581.
14. Kordower, J.H., and Bjorklund, A. (2013). Trophic factor gene therapy for Parkinson's disease. *Mov. Disord.* *28*, 96–109.
15. Goula, D., Remy, J.S., Erbacher, P., Wasowicz, M., Levi, G., Abdallah, B., and Demeneix, B.A. (1998). Size, diffusibility and transfection performance of linear PEI/DNA complexes in the mouse central nervous system. *Gene Ther.* *5*, 712–717.
16. Gwak, S.-J., Yun, Y., Yoon, D.H., Kim, K.N., and Ha, Y. (2016). Therapeutic Use of 3β-[N-(N',N'-Dimethylaminoethane) Carbamoyl] Cholesterol-Modified PLGA Nanospheres as Gene Delivery Vehicles for Spinal Cord Injury. *PLoS ONE* *11*, e0147389.
17. Kim, I.-D., Lim, C.-M., Kim, J.-B., Nam, H.Y., Nam, K., Kim, S.-W., Park, J.S., and Lee, J.K. (2010). Neuroprotection by biodegradable PAMAM ester (e-PAM-R)-mediated HMGB1 siRNA delivery in primary cortical cultures and in the postischemic brain. *J. Control. Release* *142*, 422–430.
18. Lu, S., Morris, V.B., and Labhasetwar, V. (2015). Codelivery of DNA and siRNA via arginine-rich PEI-based polyplexes. *Mol. Pharm.* *12*, 621–629.
19. Taranejoo, S., Liu, J., Verma, P., and Hourigan, K. (2015). A review of the developments of characteristics of PEI derivatives for gene delivery applications. *J. Appl. Polym. Sci.* *132*, 42096.
20. Foust, K.D., Nurre, E., Montgomery, C.L., Hernandez, A., Chan, C.M., and Kaspar, B.K. (2009). Intravascular AAV9 preferentially targets neonatal neurons and adult astrocytes. *Nat. Biotechnol.* *27*, 59–65.
21. Gholizadeh, S., Tharmalingam, S., Macaladaz, M.E., and Hampson, D.R. (2013). Transduction of the central nervous system after intracerebroventricular injection of adeno-associated viral vectors in neonatal and juvenile mice. *Hum. Gene Ther. Methods* *24*, 205–213.
22. Rao, S., Morales, A.A., and Pearse, D.D. (2015). The Comparative Utility of Viromer RED and Lipofectamine for Transient Gene Introduction into Glial Cells. *BioMed Res. Int.* *2015*, 458624.
23. Morris, V.B., and Labhasetwar, V. (2015). Arginine-rich polyplexes for gene delivery to neuronal cells. *Biomaterials* *60*, 151–160.
24. Gray, S.J., Matagne, V., Bachaboina, L., Yadav, S., Ojeda, S.R., and Samulski, R.J. (2011). Preclinical differences of intravascular AAV9 delivery to neurons and glia: a comparative study of adult mice and nonhuman primates. *Mol. Ther.* *19*, 1058–1069.
25. Bevan, A.K., Duque, S., Foust, K.D., Morales, P.R., Braun, L., Schmelzer, L., Chan, C.M., McCrate, M., Chicoine, L.G., Coley, B.D., et al. (2011). Systemic gene delivery in large species for targeting spinal cord, brain, and peripheral tissues for pediatric disorders. *Mol. Ther.* *19*, 1971–1980.
26. Brenner, M., Kisseberth, W.C., Su, Y., Besnard, F., and Messing, A. (1994). GFAP promoter directs astrocyte-specific expression in transgenic mice. *J. Neurosci.* *14*, 1030–1037.
27. Milligan, E.D., Soderquist, R.G., Malone, S.M., Mahoney, J.H., Hughes, T.S., Langer, S.J., Sloane, E.M., Maier, S.F., Leinwand, L.A., Watkins, L.R., and Mahoney, M.J. (2006). Intrathecal polymer-based interleukin-10 gene delivery for neuropathic pain. *Neuron Glia Biol.* *2*, 293–308.
28. Furman, J.L., Sama, D.M., Gant, J.C., Beckett, T.L., Murphy, M.P., Bachstetter, A.D., Van Eldik, L.J., and Norris, C.M. (2012). Targeting astrocytes ameliorates neurologic changes in a mouse model of Alzheimer's disease. *J. Neurosci.* *32*, 16129–16140.
29. Segovia, J., Vergara, P., and Brenner, M. (1998). Astrocyte-specific expression of tyrosine hydroxylase after intracerebral gene transfer induces behavioral recovery in experimental parkinsonism. *Gene Ther.* *5*, 1650–1655.
30. Kells, A.P., Fong, D.M., Draganow, M., During, M.J., Young, D., and Connor, B. (2004). AAV-mediated gene delivery of BDNF or GDNF is neuroprotective in a model of Huntington disease. *Mol. Ther.* *9*, 682–688.
31. Giralt, A., Friedman, H.C., Caneda-Ferrón, B., Urbán, N., Moreno, E., Rubio, N., Blanco, J., Peterson, A., Canals, J.M., and Alberch, J. (2010). BDNF regulation under GFAP promoter provides engineered astrocytes as a new approach for long-term protection in Huntington's disease. *Gene Ther.* *17*, 1294–1308.
32. Bordey, A., and Sontheimer, H. (1998). Electrophysiological properties of human astrocytic tumor cells In situ: enigma of spiking glial cells. *J. Neurophysiol.* *79*, 2782–2793.
33. Banner, S.J., Fray, A.E., Ince, P.G., Steward, M., Cookson, M.R., and Shaw, P.J. (2002). The expression of the glutamate re-uptake transporter excitatory amino acid transporter 1 (EAAT1) in the normal human CNS and in motor neurone disease: an immunohistochemical study. *Neuroscience* *109*, 27–44.
34. Zhang, Y., Sloan, S.A., Clarke, L.E., Caneda, C., Plaza, C.A., Blumenthal, P.D., Vogel, H., Steinberg, G.K., Edwards, M.S., Li, G., et al. (2016). Purification and Characterization of Progenitor and Mature Human Astrocytes Reveals Transcriptional and Functional Differences with Mouse. *Neuron* *89*, 37–53.
35. Godbey, W.T., Wu, K.K., and Mikos, A.G. (1999). Tracking the intracellular path of poly(ethyleneimine)/DNA complexes for gene delivery. *Proc. Natl. Acad. Sci. USA* *96*, 5177–5181.
36. Pérez-Martínez, F.C., Guerra, J., Posadas, I., and Ceña, V. (2011). Barriers to non-viral vector-mediated gene delivery in the nervous system. *Pharm. Res.* *28*, 1843–1858.
37. Lächelt, U., and Wagner, E. (2015). Nucleic Acid Therapeutics Using Polyplexes: A Journey of 50 Years (and Beyond). *Chem. Rev.* *115*, 11043–11078.
38. Newland, B., Abu-Rub, M., Naughton, M., Zheng, Y., Pinoncelly, A.V., Collin, E., Dowd, E., Wang, W., and Pandit, A. (2013). GDNF gene delivery via a 2-(dimethylamino)ethyl methacrylate based cyclized knot polymer for neuronal cell applications. *ACS Chem. Neurosci.* *4*, 540–546.
39. Horbinski, C., Stachowiak, M.K., Higgins, D., and Finnegan, S.G. (2001). Polyethylenimine-mediated transfection of cultured postmitotic neurons from rat sympathetic ganglia and adult human retina. *BMC Neurosci.* *2*, 2.
40. Tinsley, R.B., Vesey, M.J., Barati, S., Rush, R.A., and Ferguson, I.A. (2004). Improved non-viral transfection of glial and adult neural stem cell lines and of primary astrocytes by combining agents with complementary modes of action. *J. Gene Med.* *6*, 1023–1032.
41. Shi, N., Zhang, Y., Zhu, C., Boado, R.J., and Pardridge, W.M. (2001). Brain-specific expression of an exogenous gene after i.v. administration. *Proc. Natl. Acad. Sci. USA* *98*, 12754–12759.
42. Kim, B.O., Liu, Y., Ruan, Y., Xu, Z.C., Schantz, L., and He, J.J. (2003). Neuropathologies in transgenic mice expressing human immunodeficiency virus type 1 Tat protein under the regulation of the astrocyte-specific glial fibrillary acidic protein promoter and doxycycline. *Am. J. Pathol.* *162*, 1693–1707.
43. Nolte, C., Matyash, M., Pivneva, T., Schipke, C.G., Ohlemeyer, C., Hanisch, U.K., Kirchhoff, F., and Kettenmann, H. (2001). GFAP promoter-controlled EGFP-expressing transgenic mice: a tool to visualize astrocytes and astrogliosis in living brain tissue. *Glia* *33*, 72–86.
44. Lee, Y., Su, M., Messing, A., and Brenner, M. (2006). Astrocyte heterogeneity revealed by expression of a GFAP-LacZ transgene. *Glia* *53*, 677–687.
45. Ragin, A.B., Wu, Y., Gao, Y., Keating, S., Du, H., Sammet, C., Kettering, C.S., and Epstein, L.G. (2015). Brain alterations within the first 100 days of HIV infection. *Ann. Clin. Transl. Neurol.* *2*, 12–21.
46. Wang, C.Y., and Wang, S. (2006). Astrocytic expression of transgene in the rat brain mediated by baculovirus vectors containing an astrocyte-specific promoter. *Gene Ther.* *13*, 1447–1456.
47. Tripathi, S.K., Goyal, R., Ansari, K.M., Ravi Ram, K., Shukla, Y., Chowdhuri, D.K., and Gupta, K.C. (2011). Polyglutamic acid-based nanocomposites as efficient non-viral gene carriers in vitro and in vivo. *Eur. J. Pharm. Biopharm.* *79*, 473–484.
48. Goyal, R., Bansal, R., Gandhi, R.P., and Gupta, K.C. (2014). Copolymers of covalently crosslinked linear and branched polyethylenimines as efficient nucleic acid carriers. *J. Biomed. Nanotechnol.* *10*, 3269–3279.
49. Kanaan, N.M., Sellnow, R.C., Boye, S.L., Coberly, B., Bennett, A., Agbandje-McKenna, M., Sortwell, C.E., Hauswirth, W.W., Boye, S.E., and Manfredsson, F.P.

- (2017). Rationally Engineered AAV Capsids Improve Transduction and Volumetric Spread in the CNS. *Mol. Ther. Nucleic Acids* 8, 184–197.
50. Meyer, K., Ferraiuolo, L., Schmelzer, L., Braun, L., McGovern, V., Likhite, S., Michels, O., Govoni, A., Fitzgerald, J., Morales, P., et al. (2015). Improving single injection CSF delivery of AAV9-mediated gene therapy for SMA: a dose-response study in mice and nonhuman primates. *Mol. Ther.* 23, 477–487.
51. Mastorakos, P., Zhang, C., Berry, S., Oh, Y., Lee, S., Eberhart, C.G., Woodworth, G.F., Suk, J.S., and Hanes, J. (2015). Highly PEGylated DNA nanoparticles provide uniform and widespread gene transfer in the brain. *Adv. Healthc. Mater.* 4, 1023–1033.
52. Abedia (2018). *The Journal of Gene Medicine, Gene Therapy Clinical Trials Worldwide*. <http://www.abedia.com/wiley/index.html>.
53. Palfi, S., Gurruchaga, J.M., Ralph, G.S., Lepetit, H., Lavisse, S., Buttery, P.C., Watts, C., Miskin, J., Kelleher, M., Deeley, S., et al. (2014). Long-term safety and tolerability of ProSavin, a lentiviral vector-based gene therapy for Parkinson's disease: a dose escalation, open-label, phase 1/2 trial. *Lancet* 383, 1138–1146.
54. Kichler, A., Sabourault, N., Décor, R., Leborgne, C., Schmutz, M., Valleix, A., Danos, O., Wagner, A., and Mioskowski, C. (2003). Preparation and evaluation of a new class of gene transfer reagents: poly(-alkylaminosiloxanes). *J. Control. Release* 93, 403–414.
55. Morris, V.B., and Sharma, C.P. (2010). Enhanced in-vitro transfection and biocompatibility of L-arginine modified oligo (-alkylaminosiloxanes)-graft-polyethylenimine. *Biomaterials* 31, 8759–8769.
56. Gardner, J., Borgmann, K., Deshpande, M.S., Dhar, A., Wu, L., Persidsky, R., and Ghorpade, A. (2006). Potential mechanisms for astrocyte-TIMP-1 downregulation in chronic inflammatory diseases. *J. Neurosci. Res.* 83, 1281–1292.
57. Manthorpe, M., Fagnani, R., Skaper, S.D., and Varon, S. (1986). An automated colorimetric microassay for neurotrophic factors. *Brain Res. Dev. Brain Res.* 25, 191–198.